

N₂ and CO₂ vibrational modes in solid nitrogen under pressure

M. D. McCluskey^{a)}

Department of Physics and Institute for Shock Physics, Washington State University, Pullman, Washington 99164-2814

K. K. Zhuravlev

Department of Physics, Washington State University, Pullman, Washington 99164-2814

(Received 2 October 2001; accepted 31 October 2001)

Nitrogen has a complex phase diagram that has presented a formidable challenge to theoretical models. In this study, infrared (IR) spectroscopy has been performed on solid nitrogen at low temperatures and pressures up to 6 GPa. In the ϵ phase, two IR absorption peaks were observed that correspond to N–N stretch modes. The presence of two IR-active N₂ vibrons is consistent with a tetragonal structure ($P4_32_12$) and is inconsistent with an earlier proposed rhombohedral ($R\bar{3}C$) structure. The matrix isolation of CO₂ molecules in solid N₂ led to the observation of transverse (ν_2) vibrational modes, which showed a splitting consistent with the structures of the different N₂ phases. The ν_3 mode of ¹²CO₂ and ¹³CO₂ molecules was measured as a function of pressure, as well as combination modes. All the vibrational-mode frequencies shifted discontinuously at the critical pressures for N₂ phase transitions. For CO₂ concentrations of 0.1%, phase separation is present at low pressures, but is suppressed for pressures greater than 1 GPa. In summary, these studies have contributed to the knowledge of the N₂ phase diagram and the nature of guest-host interactions in molecular systems. © 2002 American Institute of Physics. [DOI: 10.1063/1.1429644]

I. INTRODUCTION

In many respects, N₂ is a model molecular system because its triple bond is very stable and its low atomic number simplifies theoretical calculations.¹ In spite of its apparent simplicity, however, N₂ has a complex phase diagram that has presented a formidable challenge to theoretical models. Theoretical studies have predicted the polymerization of nitrogen at high pressures, suggesting that nitrogen could be used as an energetic material.^{2–4} Optical and electrical studies have provided evidence that solid nitrogen becomes a nonmolecular semiconductor at pressures above 150 GPa.^{5,6} In this paper, we present the results of infrared (IR) spectroscopy measurements on N₂ under hydrostatic pressure. These studies contribute to the knowledge of the N₂ phase diagram and the nature of guest–host interactions in dense solids.

The structure of solid N₂ under hydrostatic pressure has been studied extensively by Raman spectroscopy,^{7–15} x-ray diffraction,¹⁶ and theoretical calculations^{17,18} making it an ideal system for a study of guest–host interactions. A schematic phase diagram for N₂ is shown in Fig. 1. IR spectroscopy at low temperatures and high pressures has yielded interesting results. For pressures greater than 2 GPa, an IR active N–N stretch mode, or vibron, was observed by McCluskey *et al.*¹⁹ The IR activity of this mode is due to the low symmetry of the high-pressure ϵ phase.¹¹ Subsequent investigations have measured IR-active N₂ vibrons at higher pressures.^{5,20}

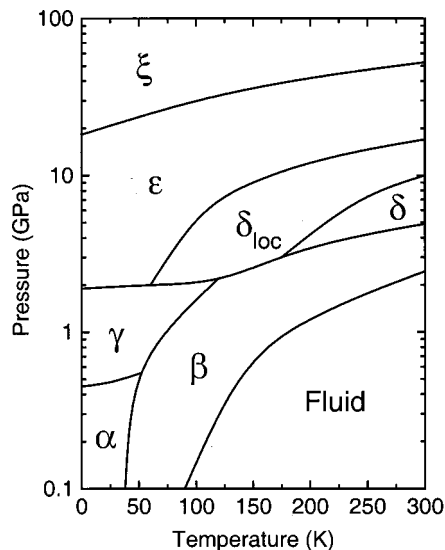
There is controversy regarding the structure of the ϵ phase. As summarized by Bini *et al.*,²⁰ theoretical studies

have predicted several different structures that appear to be at odds with experiment. An early theoretical study proposed a rhombohedral ($R\bar{3}C$) structure with eight molecules per unit cell,²¹ a model that was apparently confirmed by x-ray diffraction results.¹⁶ Subsequent calculations predicted a more complicated, tetragonal structure ($P4_32_12$) with 32 molecules per unit cell.²² The positions of the molecules in the latter structure are similar to those in the former, but their different orientations result in a lower symmetry. In this study, the results of IR spectroscopy provide evidence in favor of the tetragonal structure.

II. EXPERIMENTAL METHODS

To generate pressures up to 6 GPa, we used a piston-cylinder diamond-anvil cell.²³ Type-I diamonds with a culet diameter of 700 μm were used. After a 250 μm thick stainless steel gasket was indented to a thickness of 100 μm , a 340 μm hole was drilled in the center of the indentation. Nitrogen was used as a pressure medium and was loaded into the gasket hole by liquid immersion.²⁴ CO₂ molecules were present in the N₂ as an “unintentional” contaminant (unless indicated otherwise, the masses of C and O are 12 and 16 amu, respectively). To determine the pressure at liquid-helium temperatures, we measured the IR absorption peak of the ν_3 vibrational mode of isolated CO₂ impurities in the solid N₂ matrix. The ν_3 -mode frequency is sensitive to hydrostatic pressure²⁵ and provides a precise *in situ* pressure calibration. From the calibrated intensity of the ν_3 IR peak in solid CO₂,²⁶ the thickness of the gasket, and the intensity of the ν_3 -CO₂ peak in our measurements, the concentration of CO₂ was estimated to be 0.1% in the most heavily doped samples.

^{a)}Electronic mail: mattmcc@wsu.edu

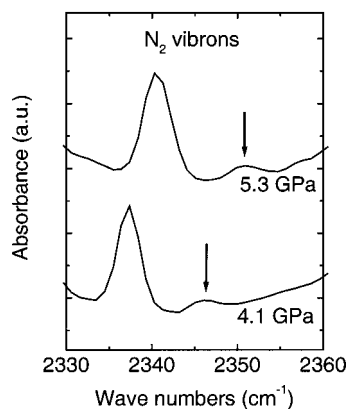
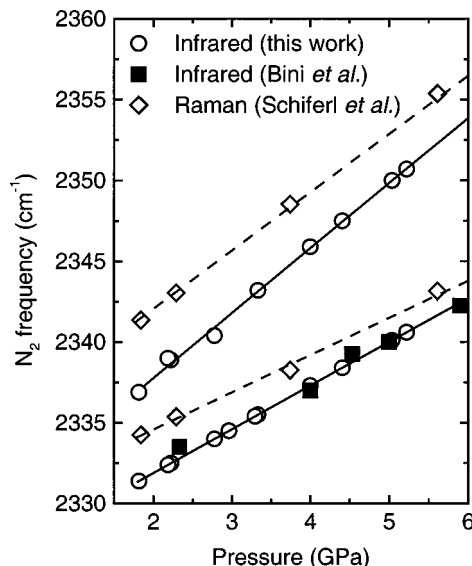
FIG. 1. Phase diagram of N₂.

Mid-IR absorption spectra were obtained with a Bomem DA8 vacuum Fourier transform spectrometer with a KBr beamsplitter. The samples were kept at a temperature of 6 to 9 K in a Janis STVP continuous-flow liquid-helium cryostat with wedged ZnSe windows. The spectral range was 500 to 5000 cm⁻¹ and the instrumental resolution was 1 to 2 cm⁻¹. An off-axis parabolic mirror and light-concentrating cone focused the light through the first diamond and onto the sample. The light then passed through the second diamond and onto a Ge:Cu photoconductor detector. After a spectrum was measured, the sample was warmed to room temperature, the pressure was adjusted, and the sample was placed back in the liquid-helium cryostat.

III. RESULTS

A. N₂ vibrons

Evidence for an additional IR-active vibron is shown in Fig. 2. In this figure, an infrared absorption spectrum is shown for two different pressures that lie within the ϵ phase. On the high-frequency side of the main N₂ vibron, a weaker peak is observed, which we attribute to a second IR-active

FIG. 2. Low-temperature IR absorption spectra of N₂ vibrons at pressures of 4.1 and 5.3 GPa. Weak peaks are indicated by the arrows.FIG. 3. N₂ vibron frequencies as a function of pressure, for low temperatures, in the ϵ phase. Circles and squares indicate IR-active vibrons measured in this work and by Bini *et al.* (Ref. 20), respectively. Diamonds indicate Raman-active vibrons measured by Schiferl *et al.* (Ref. 7). Solid lines are fits to the data (Table I) and dashed lines are guides to the eye.

vibron. The spectra shown in Fig. 2 were obtained with a spectral resolution of 2 cm⁻¹. For resolutions ≤ 1 cm⁻¹, the noise in the spectrum was high enough so that such a weak peak would not be detected. The integrated absorbance of the weak peak is approximately 7% that of the strong peak.

The N₂ vibron frequencies are plotted in Fig. 3 as a function of pressure. In this figure, IR-active vibrons observed in this work are shown by the circles. The solid lines are linear fits to the data:

$$\nu = A + BP, \quad (1)$$

where the frequency ν is in cm⁻¹ and the pressure P is in GPa. The coefficients A and B are listed in Table I for the modes measured in this work. For these N₂ vibron measurements, a sample with no detectable CO₂ was used. The pressure dependence of the main N₂ vibron was used to calibrate the pressure;¹⁹ i.e., the lower branch in Fig. 3 determines the pressure. Pieces of GaN were also in the DAC, and the pressure dependence of their two-phonon modes agreed with published data.²⁷ The solid squares are IR-active vibrons measured by Bini *et al.*,²⁰ and show good agreement with our results. The diamonds are Raman-active vibrons measured by Schiferl *et al.*⁷

In the rhombohedral $R\bar{3}C$ structure, there are two inequivalent sites, only one of which ($6e$) gives rise to an IR-active vibron.⁷ Our observation of *two* IR-active vibrons would appear to exclude the $R\bar{3}C$ structure. In the tetragonal $P4_32_12$ structure predicted by Nosé and Klein,²² nitrogen molecules reside on two inequivalent $8b$ sites (C_1 symmetry) and four inequivalent $4a$ sites (C_2 symmetry). In principle, six IR- and Raman-active vibrons should be observed, but many of these modes may be nearly degenerate or very weak. In addition, the orientations of the N₂ crystals were not well controlled. Theoretical calculations performed by Belak *et al.*¹⁸ predicted a tetragonal structure at low tempera-

TABLE I. Coefficients for the linear frequency shifts [Eq. (1)] of vibrational modes in solid N₂. The linear fits are valid for the pressure ranges indicated. The units for *A* and *B* are cm⁻¹ and cm⁻¹ GPa⁻¹, respectively.

| Mode | α phase 0–0.45 GPa | | γ phase 0.45–1.9 GPa | | ε phase 1.9–6 GPa | |
|---|------------------------------|-------------------|--------------------------------|--------------------|----------------------------------|------------------|
| | <i>A</i> | <i>B</i> | <i>A</i> | <i>B</i> | <i>A</i> | <i>B</i> |
| N ₂ vibrons | ... | ... | ... | ... | 2326.5 ^a | 2.7 ^a |
| | ... | ... | ... | ... | 2329.7±0.6 | 4.0±0.2 |
| ν_2 (CO ₂) | 662.2±0.1 | -2.6±0.3 | 662.3±0.1 | -1.9±0.1 | 661.37±0.04 | -1.15±0.01 |
| | ... | ... | 663.37±0.04 | -0.68±0.04 | 664.56±0.07 | -0.55±0.02 |
| ν_3 (¹² CO ₂) | 2349.3 ^a | 12.3 ^a | 2348.2 ^{a,b} | 7.8 ^{a,b} | 2345.1 ^a | 6.6 ^a |
| ν_3 (¹³ CO ₂) | 2283.4±0.4 | 11.7±0.9 | 2282.2±0.1 | 7.6±0.1 | 2279.4±0.2 | 6.34±0.05 |
| $\nu_3 + 2\nu_2$ (CO ₂) | 3609.6±0.1 | 9.7±0.3 | 3608.9±0.3 | 6.8±0.3 | 3604.8±0.3 | 6.7±0.1 |
| $\nu_3 + \nu_1$ (CO ₂) | 3714.0±0.3 | 13.7±0.7 | 3712.7±0.5 | 9.4±0.4 | 3706.8±0.5 | 9.4±0.2 |

^aFrom McCluskey *et al.* (Ref. 19).

^bA somewhat more precise fit is given in Ref. 19.

tures and a pressure of 7 GPa, with two vibron frequencies. These frequencies were calculated to be 2351 and 2362 cm⁻¹, in reasonable agreement with Raman spectroscopy experiments. In our work, if one extrapolates to a pressure of 7 GPa, the IR-active vibrons lie within 2 cm⁻¹ of the Raman modes, which is on the order of the uncertainty of the calculations.¹⁸ Hence, the experimental results are consistent with the theoretical predictions for the tetragonal model.

B. CO₂ transverse (ν_2) modes

As in previous work,¹⁹ we observed the antisymmetric stretching (ν_3) mode of CO₂ impurities in solid N₂ under pressure (not shown). In the present study, the higher concentration of CO₂ molecules allowed us to observe the ν_2 -mode frequencies of CO₂ impurities (Fig. 4). In the gas phase, the linear CO₂ molecule has two degenerate ν_2 modes that give rise to a single peak at 667 cm⁻¹.²⁸ These modes involve the transverse motion of the carbon atom, out of phase with the oxygen atoms. For the low-pressure α phase, only one ν_2 mode was observed. For the high-pressure phases, the interaction with the N₂ matrix lifts the degeneracy, resulting in two distinct peaks. The peaks shift discontinuously at the critical pressures for phase transitions in solid nitrogen (Fig. 5). As pressure is increased, the ν_2 modes decrease in frequency and their splitting increases.

The splitting of the ν_2 peak is consistent with the structures of the different phases. The α phase has a $Pa\bar{3}$ space group, with nitrogen molecules residing on equivalent $4a$ sites that have S_6 symmetry.⁸ Assuming the CO₂ molecules occupy substitutional sites, then the ν_2 modes are doubly degenerate. The γ phase has a $P4_2/mnm$ space group, with nitrogen molecules residing on equivalent $2a$ sites²⁹ that have D_{2h} symmetry.¹¹ In this symmetry, the degeneracy of the ν_2 modes is lifted. In the tetragonal ε phase discussed previously, there are six inequivalent sites, all of which have a low symmetry such that the ν_2 modes would be split. The fact that only two modes are observed in the ε phase suggests that the CO₂ molecules reside on one energetically preferred site.

For the highest CO₂ concentration samples, a weak peak is observed on the high-frequency side of the main ν_2 peaks, possibly a result of CO₂ dimers. For pressures less than 1 GPa, two peaks appear on the low-frequency side of the main ν_2 peaks, as indicated by the arrows in Fig. 6(a). These peaks are ascribed to ν_2 modes from solid CO₂ precipitates.

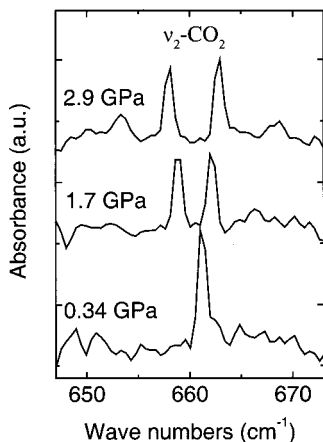


FIG. 4. Low-temperature IR absorption spectra of isolated CO₂ molecules in solid N₂, for pressures of 0.34, 1.7, and 2.9 GPa. The pressures correspond to the α , γ , and ε phases of solid N₂, respectively. The peaks are attributed to ν_2 modes of the CO₂ molecules.

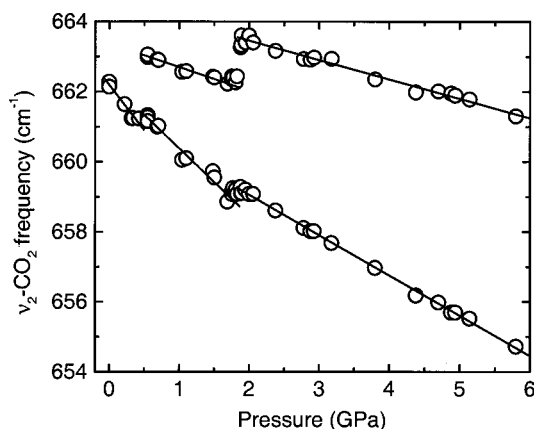


FIG. 5. ν_2 frequencies of isolated CO₂ molecules in solid N₂, as a function of pressure, at low temperatures. Discontinuous shifts of the frequencies occur at the critical pressures for phase transitions in solid N₂. Solid lines are fits to the data (Table I).

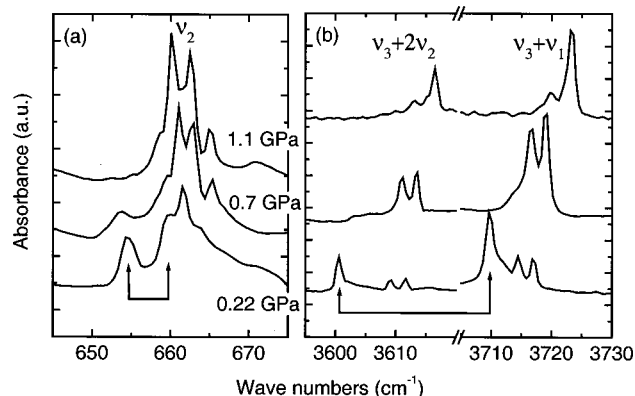


FIG. 6. Low-temperature IR spectra of CO_2 molecules in solid N_2 , at pressures of 0.22, 0.7, and 1.1 GPa. Modes arising from solid CO_2 precipitates are indicated by the arrows. (a) ν_2 frequencies of CO_2 in solid N_2 . (b) Combination-mode frequencies of CO_2 in solid N_2 .

By extrapolating the frequencies, zero-pressure values of 655 and 660 cm^{-1} are obtained, in good agreement with low-temperature IR spectra of solid CO_2 at ambient pressure.²⁶

C. CO_2 combination modes

In addition to the ν_2 and ν_3 fundamental modes, combination modes were also observed near 3600 and 3700 cm^{-1} [Fig. 6(b)]. By comparison with gas-phase data, these modes are identified as the $\nu_3+2\nu_2$ and $\nu_3+\nu_1$ combination modes, where ν_1 is the Raman-active, symmetric stretch mode. The combination modes are in Fermi resonance. In the ε phase, two IR peaks are observed. In the α and γ phases, a sideband is observed on the low-frequency side of each of the main peaks. The intensity of the sideband grows as pressure is decreased. The reason for this behavior may be related to the formation of CO_2 dimers. The combination-mode frequencies are plotted as a function of pressure in Fig. 7.

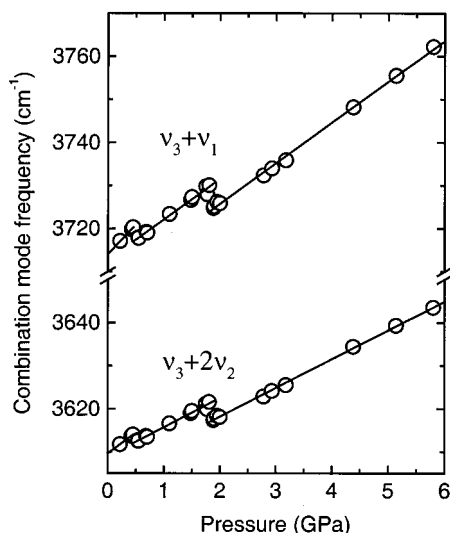


FIG. 7. Combination-mode frequencies of isolated CO_2 molecules in solid N_2 , as a function of pressure, at low temperatures. Discontinuous shifts of the frequencies occur at the critical pressures for phase transitions in solid N_2 . Solid lines are fits to the data (Table I).

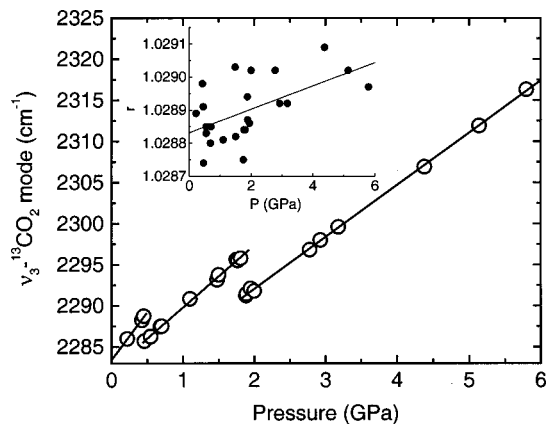


FIG. 8. ν_3 frequencies of isolated $^{13}\text{CO}_2$ molecules in solid N_2 , as a function of pressure, at low temperatures. Solid lines are fits to the data (Table I). Discontinuous shifts of the frequencies occur at the critical pressures for phase transitions in solid N_2 . The isotopic frequency ratio, $r = \nu_3(^{12}\text{CO}_2)/\nu_3(^{13}\text{CO}_2)$, is plotted in the inset.

For clarity, the low-frequency sidebands are excluded from this figure.

Along with the appearance of the solid- CO_2 ν_2 modes, solid- CO_2 peaks also appear on the low-frequency side of the combination modes, indicated by arrows in Fig. 6(b). These modes match the $\nu_3+2\nu_2$ and $\nu_3+\nu_1$ combination modes of solid CO_2 , which have frequencies of 3600 and 3708 cm^{-1} , respectively.³⁰ Since the spectroscopic signatures for solid CO_2 only occur for pressures less than 1 GPa, we conclude that phase separation of CO_2 in solid N_2 is suppressed by the application of pressure. This observation suggests that phase separation results in an increase in the total volume of the CO_2 - N_2 mixture.

D. Isotope effects

The high CO_2 concentration samples allowed us to observe the ν_3 mode of $^{13}\text{CO}_2$ molecules in solid nitrogen. This mode is plotted as a function of pressure in Fig. 8. The mode frequency increases with pressure, and decreases discontinuously at the critical pressures for solid-nitrogen phase transitions. It is apparent that $^{13}\text{CO}_2$ molecules provide a sensitive probe of the surrounding nitrogen atoms. The isotopic frequency ratio is defined as $r = \nu_3(^{12}\text{CO}_2)/\nu_3(^{13}\text{CO}_2)$, and is plotted as a function of pressure in the inset of Fig. 8. A linear fit yields a zero-pressure value of $r = 1.02883 \pm 0.00003$ and a slope of $(3.5 \pm 1.1) \times 10^{-5} \text{ GPa}^{-1}$. Given the standard error, it can be stated that the slope is greater than zero with 99.9% confidence.³¹

For a linear CO_2 molecule, in the harmonic approximation, the ν_3 -mode frequency is given by

$$\nu_3 = \sqrt{k(2/M_C + 1/M_O)} \quad (2)$$

where k is the linear force constant, M_C is the carbon mass (12 or 13 amu), and M_O is the oxygen mass (16 amu). In this model, the isotopic frequency ratio is given by $r = 1.02920$. Various anharmonic terms reduce the value of r .³² The application of pressure brings N_2 molecules closer to the CO_2

molecule, which may result in a reduction in such anharmonic terms, bringing the value of r closer to the harmonic value.

E. *Ab initio* calculations

To estimate the pressure dependence of vibrational frequencies of CO₂ molecules in solid N₂, *ab initio* calculations were performed, using GAUSSIAN 98W.³³ The restricted Hartree–Fock method was used, with the 3-21G basis set. In the α phase, N₂ molecules occupy fcc lattice sites and are oriented along the various [111] directions.³⁴ For the calculations, one CO₂ molecule was placed on a site, surrounded by twelve N₂ nearest neighbors. The position of each N atom was determined by the lattice constant a and the calculated N–N distance for an isolated N₂ molecule. While the N atoms were held fixed, the C–O bond length was optimized, to minimize the total energy. To mimic the application of pressure, lattice constants of $a=5.6, 5.4, 5.2,$ and 5.0 \AA were chosen (experimentally, $a=5.644 \text{ \AA}$).³⁵ A lattice constant of $a=5.4 \text{ \AA}$ corresponds to a pressure of approximately 0.4 GPa.³⁶ However, since our calculations do not allow relaxation of the N₂ molecules, a direct correspondence between a and pressure cannot be made. For $a=5.6 \text{ \AA}$, CO₂ frequencies of $\nu_2=661.4 \text{ cm}^{-1}$ (doubly degenerate) and $\nu_3=2471.3 \text{ cm}^{-1}$ were calculated, in good agreement with experiment. The equilibrium C–O bond length was determined to be 1.155 \AA .

As the lattice constant is decreased, the equilibrium C–O bond length decreases. The compression of the bond leads to an increase in the ν_3 -mode frequency and a decrease in the ν_2 -mode frequency. Specifically,

$$\delta\nu_2 = (1300 \pm 100)\Delta d,$$

$$\delta\nu_3 = -(10150 \pm 30)\Delta d,$$

where $\delta\nu_2$ and $\delta\nu_3$ are the frequency shifts (cm^{-1}) and Δd is the change in C–O bond length (\AA). The standard errors were obtained by linear fits to the calculated data. The ratio of the shifts is $\delta\nu_3/\delta\nu_2 = -8$. Experimentally, in the α phase, $\delta\nu_3/\delta\nu_2 = -5$, in reasonable agreement with the calculations. For the ν_3 mode, the calculated isotopic frequency ratio is $r=1.02925$ and does not vary significantly with a . Since frequencies are calculated using the harmonic approximation, this result is consistent with the hypothesis that changes in *anharmonic* terms are responsible for the experimentally observed increase in r with pressure.

IV. CONCLUSIONS

In conclusion, vibrational spectroscopy of N₂ and CO₂ in solid nitrogen under pressure has yielded information about the phase diagram of N₂ and interactions between isolated CO₂ molecules with their host environment. The presence of two IR-active N₂ vibrons in the ϵ phase is consistent with a tetragonal structure ($P4_32_12$) and is inconsistent with an earlier proposed rhombohedral ($R\bar{3}C$) structure. The transverse (ν_2) vibrational modes of CO₂ molecules showed a splitting consistent with the structures of the different N₂ phases. All the vibrational-mode frequencies shifted discontinuously at the critical pressures for N₂ phase transitions,

demonstrating that matrix-isolated molecules are sensitive probes of the host crystal. For CO₂ concentrations of 0.1%, phase separation is present at low pressures, but is suppressed for pressures greater than 1 GPa. Future studies will address the phase-separation issue in more detail and at higher pressures.

ACKNOWLEDGMENTS

The authors wish to acknowledge E. E. Haller and J. Beeman (Lawrence Berkeley National Laboratory) for providing the Ge:Cu detector and S. Watson (Washington State University) for construction of the diamond-anvil cells. This work was supported by the U.S. National Science Foundation through Grant No. DMR-9901625. Support was also provided by WSU's Institute for Shock Physics through the DOE, Grant No. DE-FG03-97SF21388.

- ¹S. Nosé and M. Klein, Phys. Rev. Lett. **50**, 1207 (1983).
- ²A. K. McMahon and R. LeSar, Phys. Rev. Lett. **54**, 1929 (1985).
- ³R. M. Martin and R. Needs, Phys. Rev. B **34**, 5082 (1986).
- ⁴C. Mailhot, L. H. Yang, and A. K. McMahon, Phys. Rev. B **46**, 14419 (1992).
- ⁵A. F. Goncharov, E. Gregoryanz, H. Mao, Z. Liu, and R. J. Hemley, Phys. Rev. Lett. **85**, 1262 (2000).
- ⁶M. I. Erements, R. J. Hemley, H. Mao, and E. Gregoryanz, Nature (London) **411**, 170 (2001).
- ⁷D. Schiferl, S. Buchsbaum, and R. L. Mills, J. Phys. Chem. **89**, 2324 (1985).
- ⁸D. Schiferl, R. LeSar, and D. S. Moore, in *Simple Molecular Systems at Very High Density*, edited by A. Polian, P. Loubeyre, and N. Boccarda (Plenum, New York, 1989), p. 303.
- ⁹M. M. Thiéry, D. Fabre, M. Jean-Louis, and H. Vu, J. Chem. Phys. **59**, 4559 (1973).
- ¹⁰S. Buchsbaum, R. L. Mills, and D. Schiferl, J. Phys. Chem. **88**, 2522 (1984).
- ¹¹F. D. Medina and W. B. Daniels, J. Chem. Phys. **64**, 150 (1976).
- ¹²R. Reichlin, D. Schiferl, S. Martin, C. Vanderborgh, and R. L. Mills, Phys. Rev. Lett. **55**, 1464 (1985).
- ¹³H. Schneider, W. Häffner, A. Wokaun, and H. Olijnyk, J. Chem. Phys. **96**, 8046 (1992).
- ¹⁴T. Westerhoff, A. Wittig, and R. Feile, Phys. Rev. B **54**, 14 (1996).
- ¹⁵M. I. M. Scheerboom and J. Schouten, Phys. Rev. Lett. **71**, 2252 (1993).
- ¹⁶R. L. Mills, B. Olinger, and D. T. Cromer, J. Chem. Phys. **84**, 2837 (1986).
- ¹⁷S. Nosé and M. Klein, Phys. Rev. Lett. **50**, 1207 (1983).
- ¹⁸J. Belak, R. Lesar, and R. D. Eters, J. Chem. Phys. **92**, 5430 (1990).
- ¹⁹M. D. McCluskey, L. Hsu, L. Wang, and E. E. Haller, Phys. Rev. B **54**, 8962 (1996).
- ²⁰R. Bini, L. Ulivi, J. Kreutz, and H. J. Jodl, J. Chem. Phys. **112**, 8522 (2000).
- ²¹R. LeSar, J. Chem. Phys. **81**, 5104 (1984).
- ²²S. Nosé and M. L. Klein, Phys. Rev. B **33**, 339 (1986).
- ²³See, for example: G. Yu. Machavariani, M. P. Pasternak, G. R. Hearne, and G. Kh. Rozenberg, Rev. Sci. Instrum. **69**, 1423 (1998).
- ²⁴D. Schiferl, D. T. Cromer, and R. L. Mills, High Temp.-High Press. **10**, 493 (1978).
- ²⁵M. D. McCluskey, L. Hsu, L. Wang, and E. E. Haller, Phys. Rev. B **54**, 8962 (1996).
- ²⁶H. Yamada and W. B. Person, J. Chem. Phys. **8**, 2478 (1964).
- ²⁷The Grüneisen parameters for the two-phonon modes were $\gamma \sim 1.4$, in agreement with single-phonon results. See A. R. Goñi, H. Siegle, K. Syassen, C. Thomsen, and J.-M. Wagner, Phys. Rev. B **64**, 035205 (2001), and references therein.
- ²⁸G. Herzberg, *Infrared and Raman Spectra of Polyatomic Molecules* (Van Nostrand, New York, 1945), p. 272.
- ²⁹*International Tables for X-ray Crystallography Vol. I* (Kynoch, England, 1952).
- ³⁰D. A. Dows and V. Schettino, J. Chem. Phys. **58**, 5009 (1973).

- ³¹P. R. Bevington, *Data Reduction and Error Analysis for the Physical Sciences* (McGraw-Hill, New York, 1969), p. 308.
- ³²A. Chedin, *J. Mol. Spectrosc.* **76**, 430 (1979).
- ³³M. J. Frisch *et al.*, GAUSSIAN 98, Revision A.9, Gaussian, Inc., Pittsburgh, PA, 1998.

- ³⁴J. A. Venables and C. A. English, *Acta Crystallogr., Sect. B: Struct. Crystallogr. Cryst. Chem.* **30**, 929 (1974).
- ³⁵L. H. Bolz, M. E. Boyd, F. A. Mauer, and H. S. Peiser, *Acta Crystallogr.* **12**, 247 (1959).
- ³⁶A. F. Schuch and R. L. Mills, *J. Chem. Phys.* **52**, 6000 (1970).